

putEMG - a surface electromyography hand gesture recognition dataset

Piotr Kaczmarek , Tomasz Mańkowski  and Jakub Tomczyński * 

Institute of Control, Robotics and Information Engineering - Poznan University of Technology, Piotrowo 3A, 60-965 Poznań, Poland; piotr.kaczmarek@put.poznan.pl (P.K.); tomasz.mankowski@put.poznan.pl (T.M.)

* Correspondence: jakub.tomczynski@put.poznan.pl; Tel.: +48-61-665-2886

Received: date; Accepted: date; Published: date

Abstract: In this paper, we present a putEMG dataset intended for evaluation of hand gesture recognition methods based on sEMG signal. The dataset was acquired for 44 able-bodied subjects and include 8 gestures (3 full hand gestures, 4 pinches, and idle). It consists of uninterrupted recordings of 24 sEMG channels from the subject's forearm, RGB video stream and depth camera images used for hand motion tracking. Moreover, exemplary processing scripts are also published. putEMG dataset is available under Creative Commons Attribution-NonCommercial 4.0 International (CC BY-NC 4.0) license at: <https://www.biolab.put.poznan.pl/putemg-dataset/>. The dataset was validated regarding sEMG amplitudes and gesture recognition performance. The classification was performed using state-of-the-art classifiers and feature sets. Accuracy of 90% was achieved for SVM classifier utilising RMS feature and for LDA classifier using Hudgin's and Du's feature sets. Analysis of performance for particular gestures showed that LDA/Du combination has significantly higher accuracy for full hand gestures, while SVM/RMS performs better for pinch gestures. Presented dataset can be used as a benchmark for various classification methods, evaluation of electrode localisation concepts, or development of classification methods invariant to user-specific features or electrode displacement.

Keywords: sEMG; dataset; gesture recognition; hand; human-machine interface; wearable

1. Introduction

Electromyography (EMG) is a well-established method of muscle activity analysis and diagnosis. A go-to approach with creating a user-friendly [human machine-interfaces \(HMIs\)](#) would be utilising the [surface electromyography \(sEMG\)](#), where non-invasive, on-skin electrodes are used to register muscle activity. Despite numerous attempts, its application in [HMIs](#) is very limited. Currently, excluding neuroprostheses, there are no commercial applications utilising interfaces based on the [EMG](#) signal. So far, the most popular attempt to commercialise [sEMG](#)-driven interface is the no longer manufactured Myo armband by Thalmic Labs, enabling recognition of few hand gestures. Several problems related to the development of interfaces of this type exist. The first crucial issue is the development of electrodes ensuring constant input impedance while providing sufficient user comfort and ease of use in conditions outside of a laboratory during prolonged usage [1–3]. Secondly, a commercial application has to meet a satisfactory level of gesture recognition accuracy, even when used by a large variety of subjects. The end-user product has to provide a low entry threshold - a long and complicated calibration procedure will discourage the user from an [EMG](#)-based [HMI](#). However, these requirements can be difficult in achieving, as the [EMG](#) signal is strongly individual [4] and non-stationary [5]. Moreover, [sEMG](#) is susceptible to external factors, such as additional mechanical loads [6–8]. Consequent re-wearing of the [sEMG](#) gesture recognition system will result in changes of the signal characteristics, as precision of electrode placement and alignment is limited for an end-user device [9,10]. In laboratory conditions, accuracy of an [HMI](#) can

be greatly improved by training the classifier for each user and each device use. Several attempts are being made to solve these problems, nonetheless, the results are not satisfactory to be implemented in an end-user device [5,8,10–12]. Potentially, modern machine learning solutions used in the analysis of images and in big data solutions, like [deep neural-networks \(DNNs\)](#), can be exploited in tasks of creating effective [sEMG](#)-based hand gesture recognition device. However, this requires availability of ready to use large data collections and processing methods. Publicly available datasets, to a large extent, contribute to accelerating this process by enabling research teams to develop and compare methods in a reliable way [13].

Several datasets containing multi-channel [sEMG](#) recordings of hand gesture executions are publicly available. Table 1 presents a summary of selected datasets with free-of-charge access. The most extensive database is the NinaPro (Non-Invasive Adaptive Hand Prosthetics) containing seven separate sets of data [14–16,23]. NinaPro DB2 [15] contains data recorded for 40 people and 52 gestures respectively, with movements tracked with CyberGlove II. Due to a large number of gestures and participants, NinaPro DB2 collection enables detection of discrete gestures, as well as development of methods for continuous joint angle estimation [24].

Most of the published [sEMG](#) datasets lack in the number of gesture repetitions, which is vital for the development of robust recognition algorithms. Moreover, when performing each gesture several times in a row (denoted in Table 1 as *repetitive*), it is likely for the subject to perform the gesture in a very similar manner. In consequence, due to a strong correlation between [sEMGs](#) signals, exceptional classification accuracy might be achieved, but significant classifier overfitting can blur the conclusions. For several datasets, gestures were executed sequentially or in random order (denoted in Table 1 as *sequential* and *random*). While both these approaches reduce the risk of a subject performing each gesture identically, it is still vital to include a large number of repetitions. Due to a number of variations that can occur in a specific gesture, repetition count as low as 10 can be insufficient, even if k-fold validation is used. IEE EMG database [18] offers the largest number of gesture repetitions, each active gesture was repeated 32 times, however, data was acquired for only four subjects. Majority of [sEMG](#) datasets contain trials recorded only during a single session. Development of an [EMG](#)-based gesture recognition system requires taking into account both [EMG](#) signal individuality and long-term variations resulting from fatigue and physiological changes. Moreover, for the end-user device, subsequent re-wearing will cause electrode misalignment. Thus, datasets containing multiple sessions will have a positive impact on such system design. Four databases listed in Table 1 contain data recorded during more than one session [10,19,21]. NinaPro DB6 [10] and Megane Pro [19] include data acquired for 10 people (7 and 15 gestures respectively), where the experiment was performed with 5-day intervals, twice each time.

Datasets listed in Table 1 represent two main measurement methods: High-Density [sEMG](#) 128-196 electrode arrays [21,22], and 10-16 electrode approach, where electrodes are often placed in anatomical points [14–19]. High-Density matrix setups provide exceptional insight into [EMG](#) signal formation processes and nature of the phenomenon, however, they are not applicable when creating portable and wearable end-user gesture recognition systems. Databases containing signals recorded from lower electrode counts, placed in sparser points, are more likely to be used in process of development of such device, as they provide signals from sensor configuration closer to a feasible end-user device. Real-time, synchronised gesture tracking is a crucial element of any usable dataset. Lack of gesture tracking during the experiment makes verification of performed gesture and proper labelling of the data difficult. Majority of datasets utilise CyberGlove II, however, glove stiffness introduces additional mechanical load to the hand, which can lead to changes in [EMG](#) signal and create a discrepancy in classifier performance, when it is applied for gesture classification performed without the glove. Despite using CyberGlove II, in most databases, data re-labelling is based on the [EMG](#) signal itself - gesture duration is detected based on the

Dataset name	EMG recording setup	Gesture tracking system	No. of participants	No. of gestures	Repetitions per session	Session count	Session organisation and intervals	Trials organisation, gesture durations
NinaPro DB1 [14]	10 sEMG ^a	yes ¹	27	52	10	1	-	random gesture: 5 s idle: 3 s
NinaPro DB2 [15]	12 sEMG ^b	yes ¹	40	49	6	1	-	repetitive gesture: 5 s idle: 3 s
NinaPro DB4 [16]	12 sEMG ^c	-	10	52	6	1	-	repetitive gesture: 5 s idle: 3 s
NinaPro DB5 [16]	16 sEMG ^d	yes ¹	10	52	6	1	-	repetitive gesture: 5 s idle: 3 s
NinaPro DB6 [10]	14 sEMG ^e	yes ²	10	7	12 [†]	10	2 per day, 5 days	repetitive gesture: 4 s idle: 4 s
NinaPro DB7 [17]	12 sEMG ^e , 9DoF IMU	-	20	40	6	1	-	sequential gesture: 5 s idle: 5 s
IEE EMG [18]	12 sEMG ^f	-	4	17	32	1	-	sequential (4 varying) no idle phase
Megane Pro [19]	14 sEMG ^e	yes ^{1,2}	10	15	12 [‡]	10	2 per day, 5 days	repetitive gesture: 8 s idle: 4 s
EMG Dataset 2 [20]	8 sEMG ^h	-	8	15	12	3	-	sequential gesture: 20 s
EMG Dataset 6 [6]	7 sEMG ^h	-	11	8	12	6	5 poses	sequential gesture: 5 s idle: 3-5s
CapgMyo(DB-a) [21]	128 HD-sEMG	-	18	8	10	1	-	repetitive gesture: 3–10 s idle: 7 s
CapgMyo(DB-b) [21]	128 HD-sEMG	-	10	8	10	2	1 day	sequential gesture: 3 s idle: 7 s
CapgMyo(DB-c) [21]	128 HD-sEMG	-	10	12	10	1	-	repetitive gesture: 3 s idle: 7 s
CSL-HDEMG [22]	192 HD-sEMG	yes ¹	5	27	10	5	different days	rsequential gesture: 3 s idle: 3 s
putEMG (this work)	24 sEMG ^g	yes ^{3,4}	44	8	20	2	1 week	sequential, repetitive gesture: 1 s or 3 s idle: 3 s

Table 1. A summary of publicly available sEMG datasets of hand gestures; the list only contains records for able-bodied subjects; biosignal recording systems: ^aOttoBock, ^bDelsys, ^cCometa, ^dThalmic Labs Myo, ^eDelsys Trigno, ^fEMG System do Brasil, ^gOT Bioelettronica MEBA, ^hDelsys Bagnoli; gesture tracking systems: ¹CyberGlove II, ²Tobii Pro Glasses 2, ³RGB HD Camera, ⁴Depth sensor - Real Sense SR300; [†]including different objects, [‡]including 2-4 different objects

onset or decay of the **EMG** signal activity [14,18]. No additional gesture tracking was used in NinaPro DB4 [16], NinaPro DB7 [17], IEE EMG [18], and CapgMyo [21] datasets.

1.1. Contribution

In this work, we would like to present the **putEMG** dataset (see Table 1 for a summary) containing **sEMG** data acquired using three 8-electrode (total of 24 electrodes) elastic bands placed around the subjects' forearm. 7 active gestures, plus an *idle* state are included in the dataset. An important advantage, compared to existing datasets, is a large number of repetitions (20) of each gesture. Data was collected for 44 participants in identical experimental procedure, repeated twice (with one-week interval) - rising the number of each gesture repetition to 40. All gestures were performed by subjects in sequential or repetitive manners, with gesture duration of 1 s and 3 s. Presented dataset can be used to develop and test user-invariant classification methods, determine features resistance to both long-term changes in the **EMG** signal and inaccurate electrode re-fitting. Usage of sparse 24 matrix-like electrode configuration enables development of methods independent from electrode placement. We also propose a novel approach to ground-truth of gesture execution, as in case of **putEMG** dataset hand movement was tracked using a depth sensor and an HD camera. Then, video stream was used for gesture re-labelling and detection of possible subjects' mistakes. In comparison to glove-like systems, this solution does not limit the freedom of hand movement and does not apply any additional mechanical load to the examined hand. **putEMG** dataset is published along with exemplary Python usage scripts allowing for fast dataset adoption.

2. putEMG data collection

2.1. Experimental setup

A dedicated experimental setup was developed for purposes of **putEMG** dataset acquisition. The setup was designed to allow for forearm muscle activity recording of a single subject with a wide range of anatomical features, especially arm circumference. Great emphasis was put on ease of use and electrostatic discharge protection as a large number of subjects participating in the experiment was planned. **putEMG** data collection bench is visible in Figure 1.

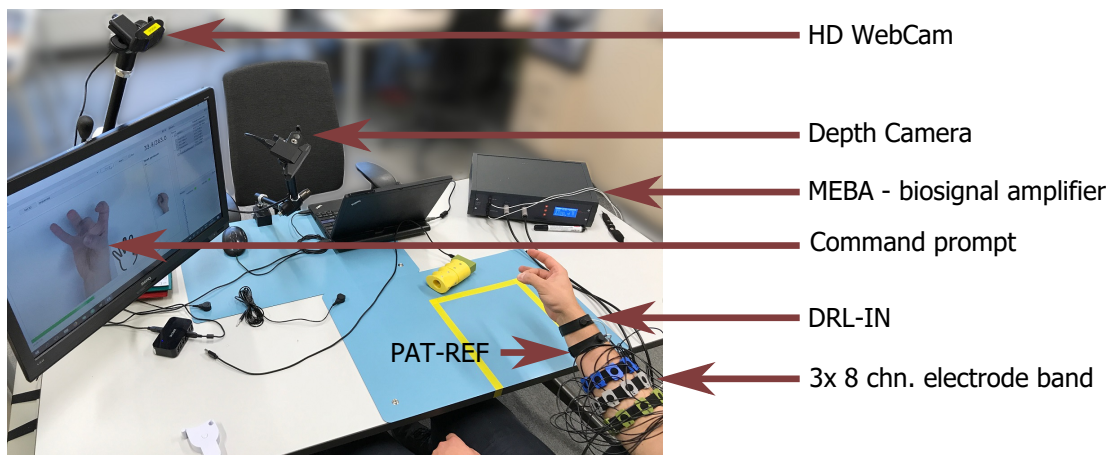


Figure 1. Setup used during acquisition of **putEMG** dataset; visible placement of **sEMG** sensor bands and reference electrodes located near the subject's wrist

For **sEMG** signal recording, a universal, desktop multi-channel biosignal amplifier, MEBA by OT Bioelettronica, was used. Data was sampled at 5120 Hz, with 12-bit **analog to digital converter (ADC)**

resolution and gain of 200. Additionally, built-in analogue band-pass filter, with a bandwidth of 3 to 900 Hz, was applied in order to eliminate bias and prevent aliasing. Signals were recorded in monopolar mode with DRL-IN and Patient-REF electrodes placed in close proximity of the wrist of the examined arm.

24 electrodes were used while recording **sEMG** signals. Electrodes were fixed around subject right forearm using 3 elastic bands, resulting in a 3×8 matrix. Bands were responsible for uniformly distributing electrodes around participant's forearm, with 45° spacing. The first band was placed in approximately $\frac{1}{4}$ of forearm length measuring from the elbow, each following band was separated by approximately $\frac{1}{5}$ of forearm length. The first electrode of each band was placed over the ulna bone and numbered clockwise respectively. Following channel numbering pattern was used: elbow band {1-8}, middle band {9-16}, wrist band {17-24}. Schematics of armbands placement is presented in Figure 2a. Different band sets were used in order to compensate for differences in participants' forearm diameter. Authors' reusable wet electrode design was used. A 3D-printed electrode allows for simple fixing to the elastic band using snap joints. Each electrode contains a 10 mm Ag/AgCl-coated element and a sponge insert saturated with electrolyte. Exploded view of the electrode design is visible in Figure 2b.

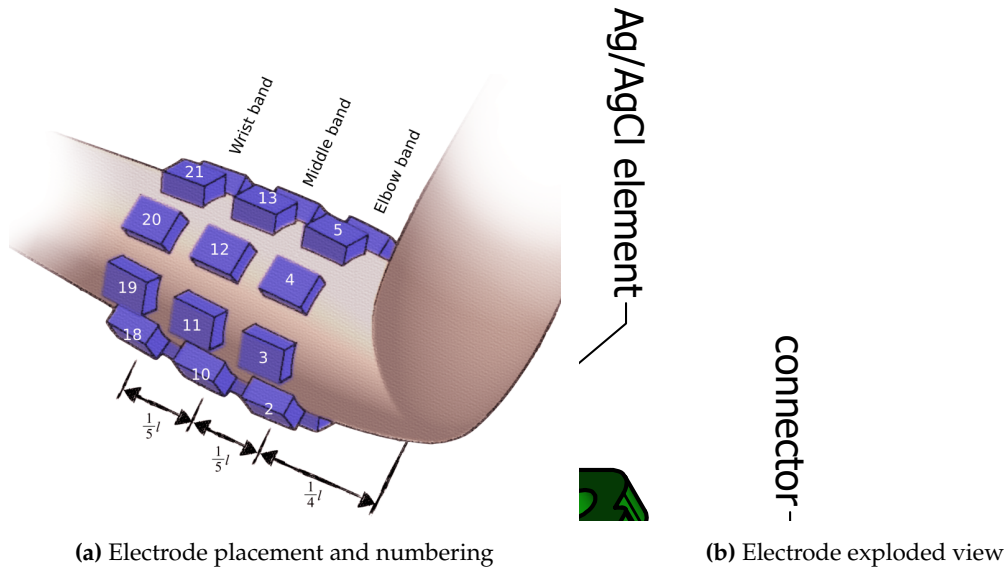


Figure 2. Schematics of electrode placement on the subject's forearm during the experiment, and design of the reusable wet electrode setup used for **putEMG** dataset experiment

Additionally, the setup included an HD Web Camera (Logitech C922) and a short-range depth sensor (RealSense SR300) with a close view of the subject's hand. Both video feed and depth images are provided alongside the **sEMG** data. These devices allow for detection of subject's mistakes, compensation of reaction time and verification of the experiment course.

2.2. Procedure

putEMG dataset consists of a series of trials that include execution of 8 hand gestures (see Figure 3). The gesture choice was based on former studies, active poses showing the highest discrimination [25–27] and best fitting for convenient **sEMG**-based **HMI** design were selected. The set consists of 7 active gestures: *fist*, *flexion*, *extension*, and 4 pinch gestures where the thumb meets one of the remaining fingers (*pinch index*, *pinch middle*, *pinch ring*, *pinch small* - Figure 3e to 3h). The 8th gesture in **putEMG** dataset is *idle*, during which subjects were asked not to move their hand, keep it in stabilised and relax muscles. A 3-second

idle period always separates execution of active gestures. Each time an active gesture was held for 1 or 3 seconds, depending on trajectory configuration. Subjects were instructed to execute all gestures with their elbow resting on the armrest with forearm elevated at a 10° – 20° angle.

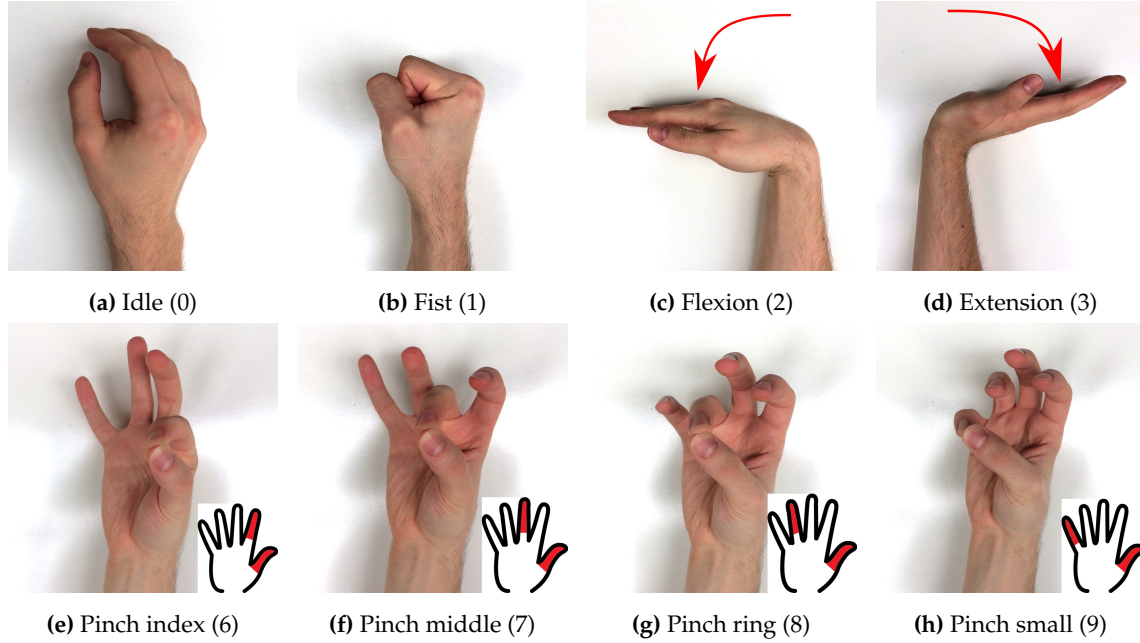


Figure 3. **putEMG** includes 8 gestures; 7 active gesture and *idle*, where subjects were asked not to move their hand; numbers in square brackets indicate gesture marker used in **putEMG** dataset files

Each experiment procedure consisted of 3 trajectories. Trajectories were divided into action blocks between which the subject could relax and move hand freely, with no restrictions. This part was introduced in order to reduce possibility of cramps and give subject a chance to rest. Each *relax* period lasted for 10 seconds and is marked with a (-1) label in **putEMG** data files. Each experiment includes the following trajectories:

- **repeats_long** - 7 action blocks, each block contains 8 repetitions of each active gesture:
[relax] 0-1-0-1-0-1-0-1-0-1-0-1-0-1-0-1-0 [relax] 0-2-0-2-0-2-0-2-0-2-0-2-0-2-0-2-0 [relax] 0-3-0... ,
- **sequential** - 6 action blocks, each block is an subsequent execution of all active gestures:
[relax] 0-1-0-2-0-3-0-6-0-7-0-8-0-9-0 [relax] 0-1-0-2-0-3-0-6-0-7-0-8-0-9-0 [relax] 0-1-0-2-0... ,
- **repeats_short** - 7 action blocks, each block contains 6 repetitions of each active gesture:
[relax] 0-1-0-1-0-1-0-1-0-1-0-1-0 [relax] 0-2-0-2-0-2-0-2-0-2-0-2-0 [relax] 0-3-0... .

This results in 20 repetitions of each active gesture in a single experiment performed for one participant. Each subject performed the experiment twice with at least one-week time separation, raising the number of active pose repetitions to 40. However, electrode band placement repeatability is not completely ensured and could differ slightly between experiments.

Suitable PC software was created in order to guide the participant through the procedure and record data. During the experiment, the subject was presented with a photo of the desired gesture to be performed (see Figure 3). The software also provided a preview of the next gesture and countdown to next gesture transition. Before each experiment, the subject performed a familiarisation procedure, which is not included in the dataset.

2.3. Participants

Each subject signed a participation consent along with data publication permit. Before the first experiment, each participant filled a questionnaire that included: gender, age, height, weight, dominant hand, health history, contact allergies, sports activity, and tobacco usage. Additionally, forearm diameter was measured in places where wrist and elbow bands were placed. Anonymous questionnaires are published along with **putEMG** dataset. The study was approved by the Bioethical Committee of Poznan University of Medical Science under no 398/17.

putEMG dataset covers 44 healthy, able-bodied subjects - 8 females and 36 males, aged 19 to 37. As described in Section 2.2, each participant performed the experiment twice.

2.4. Pre-processing and labelling

Published **sEMG** data was not altered by any means of digital signal processing. Signals provided in **putEMG** dataset are raw **ADC** values, not filtered or trimmed. Each trial is an uninterrupted signal stream, that includes all trajectory parts: steady states and transitions. If needed, **sEMG** signal can be converted to millivolts using the following formula:

$$x = \frac{N \cdot 5}{2^{12}} \cdot \frac{1000}{200} [mV], \quad (1)$$

where N is a raw **ADC** value stored in **putEMG** files.

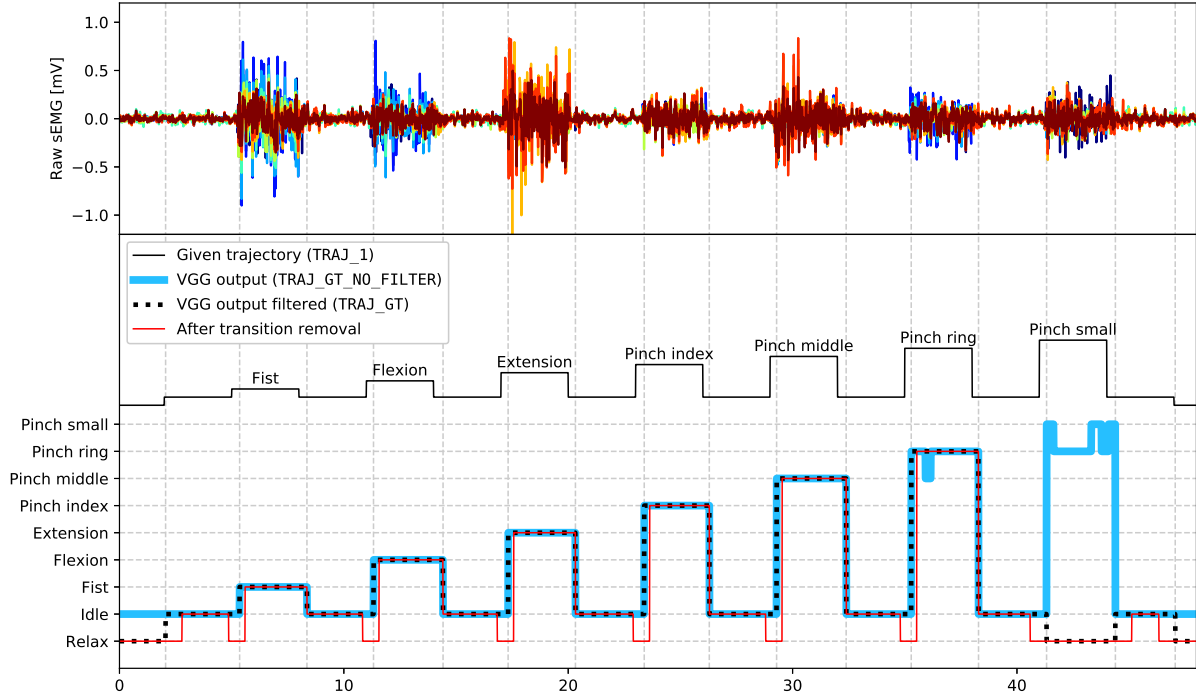


Figure 4. Exemplary fragment of ground-truth label processing stages; *fist - pinch middle*: gestures were performed and recognised properly, only transition points were adjusted; *pinch ring*: gesture was mostly recognised as correct, mistakes in *VGG output* were filtered; *pinch small*: gesture was mostly recognised as incorrect, whole gesture was rejected; vertical grid corresponds to transitions in *VGG output filtered*

sEMG data is labelled by a trajectory that was presented to participants during experiments (**TRAJ_1** column in the dataset), with gestures labelled with numbers presented in Figure 3 (*relax* periods are marked as (-1)). However, as gesture execution may not perfectly align to given trajectories, due to the subjects' delay in command performance or mistakes, all gestures were relabelled based on the captured video stream. VGGNet [28], a convolutional neural network, was trained and applied to video gesture recognition with 98.7% accuracy (saved as **TRAJ_GT_NO_FILTER** column). Afterwards, output from the neural network was filtered using a median filter and then referenced to given trajectory values. Each gesture execution was allowed to begin 250 ms earlier than given user prompt, and end 2000 ms later than the next prompt appeared. Any occurrences of a gesture outside of these boundaries were trimmed. Contradictory labels (where most of a particular gesture occurrence was recognised as mistaken) were labelled as (-1), marking them not to be processed. As participants could notice and try to correct the mistake mid-execution, which would cause abnormal muscle activity, the whole gesture occurrence is rejected. Filtered VGGNet gesture ground-truth were put into **TRAJ_GT** column. Example of ground-truth trajectories placed side by side with corresponding **EMG** recordings are presented in Figure 4.

putEMG dataset is available under Creative Commons Attribution-NonCommercial 4.0 International (CC BY-NC 4.0) license at: <https://www.biolab.put.poznan.pl/putemg-dataset/>. For more detailed information on data structures and handling see Appendix A.

3. Technical validation

This section presents the validation of **putEMG** dataset properties. Recorded **sEMG** signals were assessed in respect of their usefulness. Well established state-of-the-art classification methods and feature sets were examined as a baseline for future applications.

3.1. Amplitudes assessment

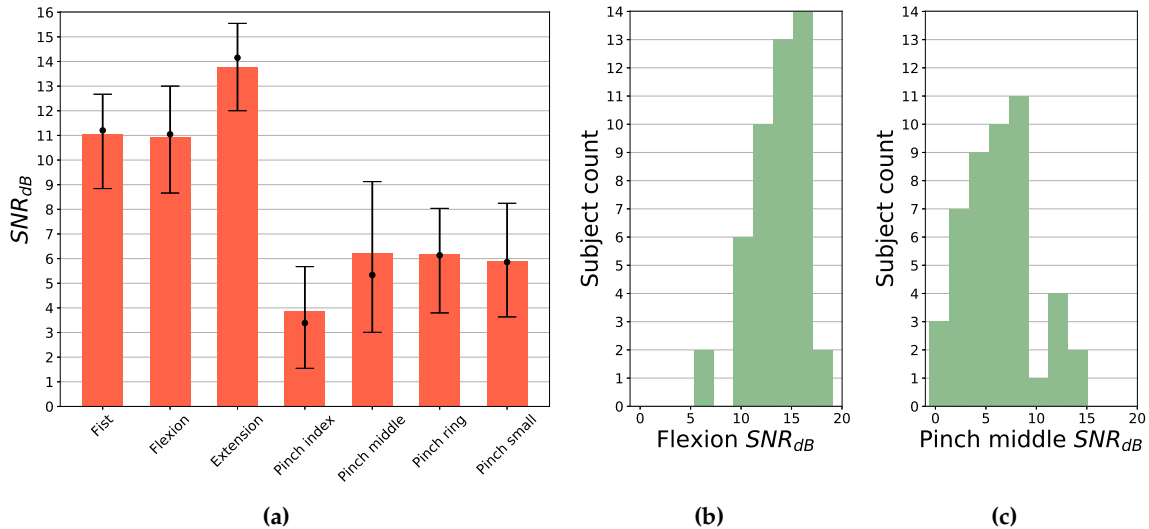


Figure 5. Signal-to-noise ratio (SNR) analysis of gesture execution; all values were calculated relative to *idle* period, in this case considered as noise; for each gesture type SNR was averaged over 5 most active channels; (a) SNR by gesture; bars represent mean value; dot marks SNR median value together with 25th and 75th percentile; (b) Histogram of SNR for *flexion* gesture; (c) Histogram of SNR for *pinch middle* gesture

Many factors affecting **sEMG** signal variability exist. Across subject population, main differences include skin-electrode contact impedance, the thickness of fat tissue, and diversity in muscle activity level.

A common approach in most [EMG](#) processing methods, to avoid the above issue, is signal normalisation with respect to [Maximum Voluntary Contraction \(MVC\)](#) [29] or another reference activity [4]. In this work, [sEMG](#) amplitudes are characterised as a ratio of signal power during active gestures with respect to *idle*, expressed as [SNR](#). This allows for direct comparison between signals in *idle* and during active gesture performance, which is crucial for classification purposes. The [SNR](#) is given by the formula:

$$SNR_{dB} = 20 \cdot \log \left(\frac{P_{gesture}}{P_{idle}} \right), \quad (2)$$

where $P_{gesture}$ is the average signal power of active gesture, P_{idle} refers to signal power in *idle* state. Respective signal sections were selected using trajectory after label processing and transition removal. [SNR](#) results per gesture averaged across 5 most active channels in each gesture are presented in Figure 5a. *Extension* gesture generates significantly ($p < 0.05$) higher activity than other hand movements, for the majority of subjects averaged [SNR](#) is calculated above 14 dB. [SNR](#) for *fist* and *flexion* is recorded above 11 dB, while for pinch gestures [SNR](#) is significantly lower, with median value falling in the range of 3 to 6 dB. Histograms of [SNR](#) for two substantially different gestures (*flexion* and *pinch middle*) are presented in Figure 5b and 5c, presenting quasi-normal distribution. However, distribution parameters differ significantly ($p < 0.05$). Smallest observed *flexion* gesture [SNR](#), for most subjects, is above 10 dB. Only for 2 participants it has fallen below 10 dB. In case of *pinch middle* gesture, for 3 subjects, [SNR](#) value was recorded below 0 dB. In case of these participants, manual analysis of raw [sEMG](#) signals and video footage showed abnormal activity during *idle* stage, caused by excessive forcing of finger extension during these periods. In general, for all pinch gestures, lower [SNR](#) was observed. It is due to a smaller count of muscles being activated during these gestures, causing fewer channels to present high activity.

3.2. Feature extraction and classification benchmark

The advantages of [putEMG](#) dataset are a large number of subjects and a larger number of gesture repetitions compared to other publicly available datasets. The dataset can be used to develop classification methods or to extract or test subject-invariant features. Therefore, in this work, we present the performance of state-of-the-art classification methods and feature sets.

3.2.1. Used feature sets and classifiers

So far, many approaches were presented to [EMG](#) feature extraction and classification [8,30]. For this work, three most popular feature sets were selected: [Root Mean Square \(RMS\)](#), [Hudgins' feature set](#) [31] and [Du's feature set](#) [32]. [Hudgins' set](#) consists of [Mean Absolute Value \(MAV\)](#), [Waveform Length \(WL\)](#), [Zero Crossing \(ZC\)](#), and [Slope Sign Change \(SSC\)](#). It is characterised by relatively high classification accuracy, high insensitivity to window size, and low computational complexity [33]. [Du's feature vector](#) is composed of [integrated Electromyogram \(iEMG\)](#), [variance \(VAR\)](#), [WL](#), [ZC](#), [SSC](#) and [Willison Amplitude \(WAMP\)](#). In some research, it is reported to present higher performance than [Hudgins' set](#) [30]. Even though [Hudgins' and Du's sets](#) are computed in the time domain, they represent amplitude, frequency, and complexity of the signal [8]. The gesture classification was performed using four different classifiers: [Linear Discriminant Analysis \(LDA\)](#), [Quadratic Discriminant Analysis \(QDA\)](#), [k-nearest Neighbours Algorithm \(kNN\)](#) and [Support-Vector Machine \(SVM\)](#) (with [radial basis function \(RBF\)](#) kernel), which are commonly used in [EMG](#) classification tasks [6,8,30,32]. Besides well-established, classic classification approaches, a number of attempts use [DNNs](#) [13]. In order to compare results generated by [DNNs](#), all hyperparameters, network topology, and training scheme has to be reproduced. Unfortunately, networks architecture and hyperparameters values cannot be simply deduced from most of the manuscripts. In this article, a comparative benchmark using [DNN](#) was not performed.

3.2.2. Classification pre-processing and data split

Solely for classification purposes, raw sEMG data was filtered using a bandpass filter with cutoff frequencies of 20 and 700 Hz. Furthermore, to reduce interference generated by the mains grid and other equipment used during the experiment, an adaptive notch filter attenuating frequencies of 30, 50, 90, 60, and 150 Hz was applied. Filtered sEMG signal was used to calculate features needed for feature sets described in Section 3.2.1. A moving window of 5000 samples (488 ms) and step of 2500 samples (244 ms) was used during the above calculations. Gesture ground-truth label for calculated features was sampled at the end of the processing window. In addition to initial label pre-processing described in Section 2.4, the gesture trajectories were further trimmed to exclude transitions between *idle* and active gesture: 488 ms before the gesture start and 244 ms after the gesture start (see *After transition removal* plot in Figure 4). Trimming periods correspond to analysis window length and step used in feature calculation, as each feature sample is computed using past raw data.

Each participant's data, from each experiment day, was processed separately generating 88 independent subsets. Among each subset, three trials were present, as described in Section 2.2. These trials were divided into training and test datasets, generating 3-fold validation splits, where two trials were concatenated to generate a training set and the remaining trial was used as a testing set.

3.2.3. Classification performance

This section presents a comparison between different combinations of classifiers and feature sets, all differences described here are significant with a probability value of $p < 0.05$. Significance of classifier mean accuracy comparisons was evaluated using ANOVA and Tukey's tests. Precision, recall, and accuracy were calculated for each class separately and averaged with equal weights.

Used classifiers' hyperparameters were empirically tuned in order to minimise the difference in accuracy between training and test sets. For SVM classifier, C parameter of the RBF kernel can be treated as regularisation parameter tuning decision function's margin. Large values of C will reduce acceptance margin, while lower values will promote wider margin and in consequence, generate a simpler decision function. In this work, $C = 50$ was selected. kNN k parameter reflecting the number of neighbouring samples was set to 5. For QDA, classifier covariance estimate regularisation parameter was equal to 0.3. In case of default parameters for SVM ($C = 1.0$), underfitting was observed, while for QDA (regularisation parameter equal to 0.0), the results were overfitted.

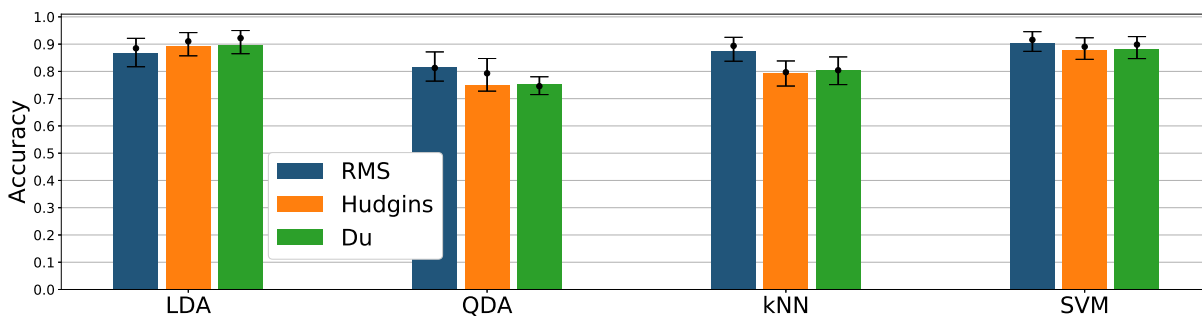


Figure 6. Classification accuracy for different classifiers and feature sets combinations; bars represent mean value; dots mark accuracy median value together with 25th and 75th percentile; results presented for 24 channel configuration

Among tested classifier and feature sets, the highest overall mean accuracy was achieved by LDA/Hudgins, LDA/Du, and SVM/RMS combinations (89 - 90%, see Figure 6), differences between them are insignificant. For RMS feature, the accuracy of SVM is better (90%) than for LDA, kNN, and QDA (86%,

87%, 81% respectively). Difference between **kNN** and **LDA** is negligible (Figure 6). Accuracies achieved for Hudgins' and Du's feature sets within a single classifier are very similar, however, results between various classifiers fed with Hudgins' or Du's sets differ significantly. For **QDA**, **kNN**, and **SVM** classifiers, combined with the **RMS** feature, accuracy presents exceeding performance (81%, 87%, 90% respectively) compared with other features sets (74%, 78%, 87%). Unlike other classifiers, **LDA** presents higher accuracy for Du's and Hudgins' feature sets (88% and 89%) than for **RMS** (Figure 6).

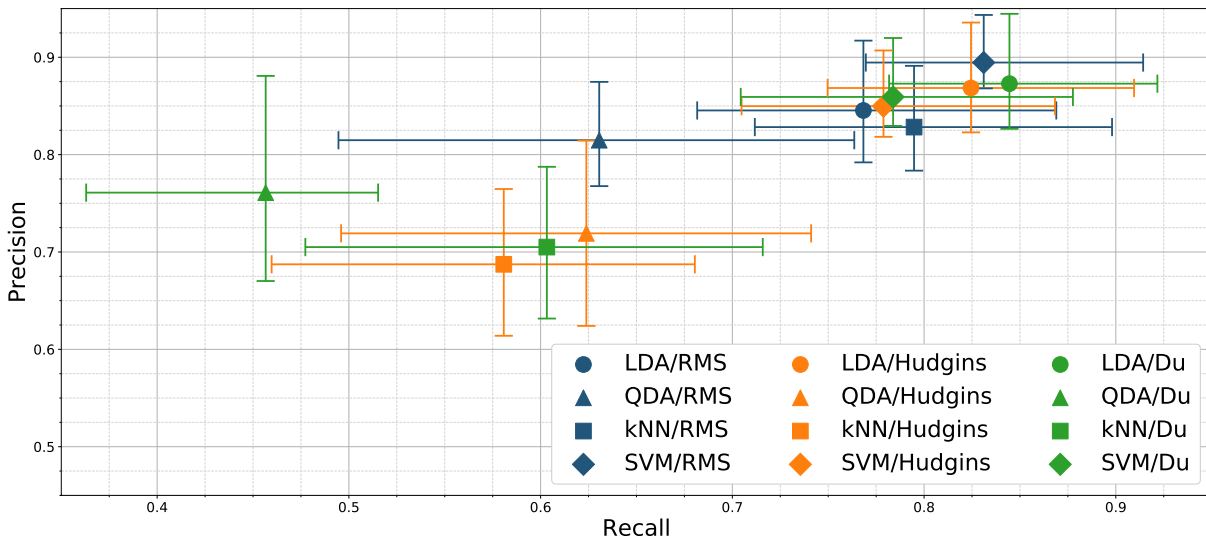
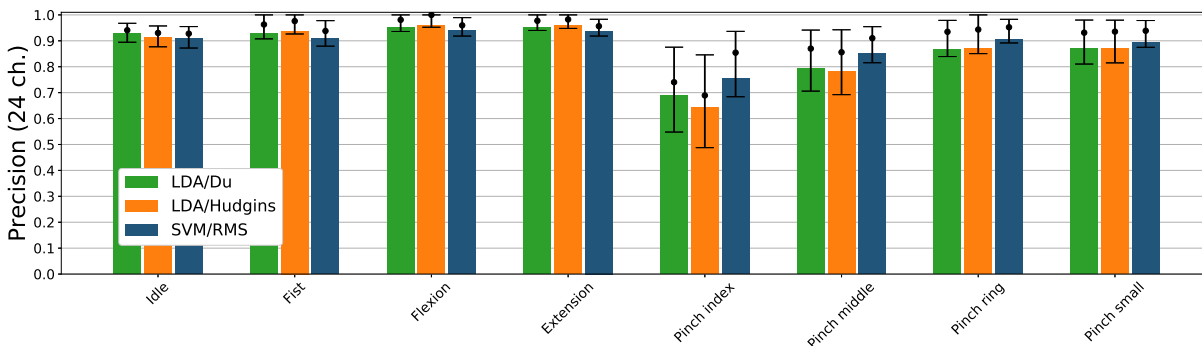


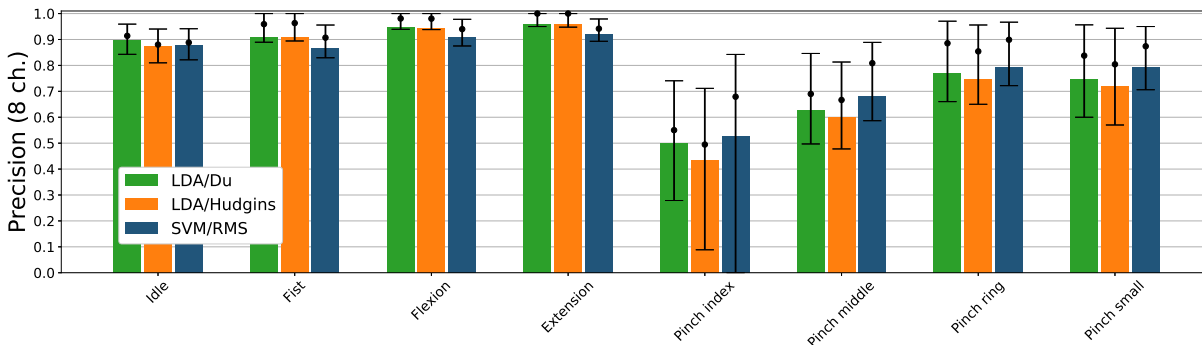
Figure 7. Classification precision and recall mean relationship for different classifiers and feature sets combinations; error bars mark 25th and 75th percentile; results presented for 24 channel configuration

Figure 7 presents resulting precision-recall relationship of tested classifiers and feature sets combinations. **LDA/Du** and **LDA/Hudgins** combinations display similar performance, significantly different than all remaining classifiers. Highest precision score (89%) is presented by **SVM/RMS**. Additionally, the precision scores of **LDA/Du** and **LDA/Hudgins** are insignificantly different with respect to **SVM/Du**, **SVM/Hudgins**, and **LDA/RMS**. The highest recall was achieved for **SVM/RMS**, **LDA/Du** and **LDA/Hudgins** (83%, 84%, 82%).

Figure 8 presents precision score with respect to each gesture and electrode setups consisting of 24 and 8 **sEMG** channels. Results are presented only for three classifier and feature set combinations showing the highest accuracy (see Figure 6). Considering 24 electrode configuration (Figure 8a), **LDA/Du** composition has higher precision (92%) for *idle* than other considered classifiers (90 - 91%). **LDA/Du** and **LDA/Hudgins** present similar precision for *fist*, *flexion* and *extension* gestures (93%, 95%, 95%) than **SVM/RMS** (91%, 93% and 93%). Conversely, **SVM/RMS** has a higher precision score for *pinch index*, *pinch middle* and *pinch ring* gestures (75%, 85%, 90%) than **LDA/Du** or **LDA/Hudgins** (68%, 79%, 87%). The differences in precision score classification for *pinch small* gesture are insignificant (89 - 86%). For all classifiers, the lowest precision is achieved for *pinch index* gesture. In case of 8 **sEMG** channel configuration (middle electrode band, Figure 8b), *idle* state is detected with lower precision than for 24 channels setup, **LDA/Du** combination remains better performing (89%) compared to all other classifier and feature sets. For remaining gestures, differences between **LDA/Du** and **LDA/Hudgins** are insignificant. These classifiers perform with higher precision while detecting *fist*, *flexion* and *extension* gestures (90%, 94%, 96%) compared to combinations including **SVM** (86%, 90%, 92%). For pinch gestures, the highest precision is presented by **SVM/RMS** (52%, 68%, 79%, 79%), however compared to **LDA/Du**, the difference is insignificant (49%, 62%, 77%, 74%). Precision for **LDA/Hudgins**, in case of pinch gestures, is lower than for **SVM/RMS**.



(a) 24-channel electrode configuration



(b) 8-channel electrode configuration (middle electrode band)

Figure 8. Classification precision for selected classifiers and feature sets combinations, presented for each active gesture in **putEMG** dataset; bars represent mean value; dots mark precision median value together with 25th and 75th percentile

The decay in precision between 24 and 8 channel configurations for *fist*, *flexion* and *extension* gestures is insignificant when considering **LDA** classifiers, although it is notable for **SVM/RMS** combination in 24 electrode setup. Still, an absolute decrease in precision is smaller than 5%. For all classifiers, decay in precision for pinch gestures classification can be observed (10 - 23%).

4. Discussion

Mean signal powers averaged across all records reveal that *fist*, *flexion* and *extension* generate stronger activity than pinch gestures, by more than 4 dB. Significant differences in amplitudes between tested gestures were also reported by Phinyomark et al. [34], but in contrast to our results, *fist* gesture generated significantly stronger activity than *flexion* or *extension*. Contrary to all above, results from NinaPro dataset did not reveal significant differences in amplitudes with respect to gestures [14]. The origin of these discrepancies is ambiguous. In the case of NinaPro dataset, a higher activity might be induced by the stiffness of CyberGlove II, whereas in the case of **putEMG** dataset, hand motion was not obstructed. Another possible explanation is differences in experimental procedure and data processing. In contrast to NinaPro, in our experiment, the elbow was always supported. Moreover, our results are presented as **SNR** with respect to *idle* state, and therefore activity generated by the gravitational load is filtered out, while in NinaPro observed activity contains both the component caused by volatile movement and hand weight compensation.

A significant difference between pinch gestures and other gestures is observed in both signal amplitudes, and classification results. Individual finger motion generates significantly smaller muscle

engagement than full hand motions, **EMG** activity area is also limited [35]. Therefore, for distinguishing between pinch gestures, methods able to map arbitrary regions of activity may be more feasible. It might explain why **SVM/RMS** performs better for pinch gestures than **LDA**, even when the latter uses more complex feature sets. **SVM** is able to generate more complex decision boundary to distinguish between different spatial activity patterns, compared to **LDA**. In this case, richer information related to muscle activity, presented by Du's or Hudgins' feature sets, is less beneficial than complex spatial decision boundary. This statement can also be proven by significant degradation of **SVM/RMS** precision when only 8 electrodes are considered.

Based on the ROC curve for a given classifier, precision and recall are dependent in the sense that increasing one of these measures decreases the other one. Even though Figure 7 does not present ROC curves, but only single points referring to classifier/feature set configurations, it can be deduced that **SVM/RMS**, **LDA-Hudgins**, and **LDA/Du** setups perform better than other classifiers. Based on overall accuracy, none of them can be pointed out as superior at a significant level ($p < 0.05$). Precision scores calculated for each gesture separately reveal that **LDA/Du** is superior for classification of *idle*, *fist*, *flexion*, and *extension*, while **SVM/RMS** performs better for pinch gestures.

Reported **putEMG** gesture classification performance is lower than results presented in similar works, where **sEMG** signals were recorded for smaller groups of subjects [6,8,36–38]. Kushaba et al. [6] analysed only full hand movements and *pinch index* gesture and reported highest accuracy (98 – 99%) for **SVM** classifier, depending on the subject's pose, and 97 – 99% with **LDA**. Al-Timemy et al. [36] analysed individual finger motions and reported classification accuracy of over 98% for 5 classes and over 90% for 12 classes. With **putEMG** overall accuracy of 90% was achieved. The discrepancies can be explained in several ways. In the aforementioned works, different feature vectors were used, and **Orthogonal Fuzzy Neighbourhood Discriminant Analysis (OFNDA)** dimensionality reduction method was applied. In our results, the dimensionality reduction issue is omitted, as the classification is performed as technical validation of **putEMG** dataset. In works mentioned above, dimensionality reduction was performed for each training set separately, which could lead to drawing improper conclusions regarding full dataset. The second crucial difference is the number of subjects and the experimental procedure. In the case of [6,8,36–38], no more than 10 subjects participated in the experiment. In broader datasets, there is a higher chance that subjects participated in such study for the first time, therefore the diversity of the group may be higher and degrade overall accuracy. As can be seen in Figures 8a, 8b, median precision values are higher than reported mean values, with mean values often closer to the 25th percentile, suggesting the drop in average performance caused by individual subjects. Gesture diversity also has a high impact on obtained results. In presented dataset validation, both individual finger gestures and full hand movements are recognised by a common classifier, while in mentioned experiments, they were processed separately. A higher number of gesture classes may cause accuracy decay. For instance, in the case of NinaPro DB5 dataset and 41 gesture classes, reported accuracy was 74% [16].

RMS feature performs better with **QDA**, **kNN**, and **SVM** classifiers due to the low size of input vector ($24 \cdot 1$), while Hudgins, and Du sets consist of $24 \cdot 4$ and $24 \cdot 6$ features, respectively. Tested classifiers differ in the complexity of the decision boundary, and in the number of parameters to be estimated during the training process. In the case of **LDA**, the number of parameters is the lowest and proportional to the number of inputs. For **QDA** covariance is estimated separately for each class and the number of parameters is quadratic in relation to input vector size. In the case of **kNN**, the number of parameters affects metric confidence, as features are not weighted with respect to their decisive importance. It indicates the necessity of dimensionality reduction of the input feature set before the classification.

After tuning, hyperparameters values revealed that regularisation is required to avoid overfitting. Nevertheless, the selected number of **kNN** neighbours is 5, a low value considering 8 gestures and at least 10000 samples per gesture in the training set. In the case of **SVM**, the C parameter had to be set to a high

value promoting small margins and more complex decision boundary. These facts might indicate that the dataset is highly diverse. It might be thanks to the procedure consisting of gestures performed both in sequences and consecutive repeats, and variable gesture durations.

5. Conclusions

This paper presents a **sEMG** signal dataset intended for hand gesture recognition purposes, acquired for 44 able-bodied subjects performing 8 different gestures (including *idle* state). A publicly available **putEMG** dataset is aimed to be a benchmark for classification approach comparison and as a test bench for evaluation of different aspects of wearable **sEMG**-based **HMI**s, such as electrode configurations, robustness improvement, or armband localisation changes. The most significant advantage of presented **putEMG** dataset is a large group of participants performing a high number of gesture repetitions compared to similar works [8,14,14,18]. High gesture performance diversity was assured by including both repetitive and sequential gesture execution procedure with varying duration. The dataset also introduces a novel approach to gesture execution ground-truth by utilising an RGB video stream and a depth camera.

The dataset validation, using state-of-the-art classification methods, demonstrated acceptable classification accuracy of approximately 90% (for **SVM/RMS**, **LDA**/Hudgins and **LDA**/Du classifier and feature set combination). Although this result is worse than those presented in related work, it was achieved for a larger and highly diverse group of participants. Moreover, dimensionality reduction was not applied, which might also affect classification performance. It should be underlined that the main aim of this article was to present the dataset, and classification results have to be treated as a baseline for characterising **putEMG** data quality, and not classifier performance itself. Obtained results indicate that **putEMG** can be successfully used as a benchmark for wearable, end-user hand gesture recognition systems development.

Author Contributions: Conceptualization, Piotr Kaczmarek; Data curation, Tomasz Mańkowski and Jakub Tomczyński; Formal analysis, Piotr Kaczmarek; Funding acquisition, Jakub Tomczyński; Investigation, Piotr Kaczmarek, Tomasz Mańkowski and Jakub Tomczyński; Methodology, Piotr Kaczmarek; Project administration, Jakub Tomczyński; Software, Tomasz Mańkowski and Jakub Tomczyński; Validation, Piotr Kaczmarek; Visualization, Tomasz Mańkowski; Writing – original draft, Piotr Kaczmarek, Tomasz Mańkowski and Jakub Tomczyński; Writing – review & editing, Tomasz Mańkowski and Jakub Tomczyński.

Funding: The work reported in this paper was partially supported by a grant from the Polish National Science Centre, research project no. 2015/17/N/ST6/03571.

Conflicts of Interest: The authors declare no conflict of interest.

Abbreviations

ADC analog to digital converter.

CSV comma-separated values.

DNN deep neural-network.

EMG electromyography.

HDF5 Hierarchical Data Format 5.

HMI human machine-interface.

iEMG integrated Electromyogram.

kNN k-nearest Neighbours Algorithm.

LDA Linear Discriminant Analysis.

MAV Mean Absolute Value.

MVC Maximum Voluntary Contraction.

OFNDA Orthogonal Fuzzy Neighbourhood Discriminant Analysis.

QDA Quadratic Discriminant Analysis.

RBF radial basis function.

RMS Root Mean Square.
sEMG surface electromyography.
SNR signal-to-noise ratio.
SSC Slope Sign Change.
SVM Support-Vector Machine.
VAR variance.
WAMP Willison Amplitude.
WL Waveform Length.
ZC Zero Crossing.

Appendix A. putEMG dataset structure and handling

Full **putEMG** dataset data structure description along with database hosting address is provided at <https://www.biolab.put.poznan.pl/putemg-dataset/>. **putEMG** dataset is available in two file formats: **Hierarchical Data Format 5 (HDF5)** (recommended to be used with pandas - Python Data Analysis Library) and **comma-separated values (CSV)** (additionally zipped in order to reduce size).

All record filenames use the following format:

`emg_gesture-<subject>-<trajectory>-<YYYY-MM-DD-hh-mm-ss-milisc>`,
 where:

- `<subject>` – two-digit participant identifier,
- `<trajectory>` – trajectory type: `repeats_long`, `sequential`, `repeats_short`,
- `<YYYY-MM-DD-hh-mm-ss-milisc>` - time of experiment start in stated format.

Independent from file format, each record includes following columns:

- **Timestamp**,
- **EMG_1...EMG_24** - **sEMG** raw **ADC** samples - column numbers explained in Section 2.1 and Figure 2a,
- **TRAJ_1** - label representing command shown to the subject during the experiment,
- **TRAJ_GT_NO_FILTER** - gesture recognised from the video stream, not processed,
- **TRAJ_GT** - ground-truth estimated from the video stream, processed as described in Section 2.4,
- **VIDEO_STAMP** - frame timestamp in the corresponding video stream.

All records are accompanied with 1080p and 576p, 30 fps video streams in H264 MP4 format, and depth camera images in PNG format with a resolution of 640×480 px and 60 fps. Depth camera images are named `depth_<timestamp>.png`, with `<timestamp>` in the time domain of corresponding record file (in milliseconds), and put into a zip archive. Both video streams and depth images archive filenames follow the same scheme as corresponding record filenames.

When downloading **putEMG** dataset it is highly recommended to use an automated Python or Bash script available at GitHub repository: <https://github.com/biolab-put/putemg-downloader>

Examples of **putEMG** usage are provided in another GitHub repository: https://github.com/biolab-put/putemg_examples. In order to reproduce the results from this work, run `shallow_learn.py` example from the above repository.

References

1. Roland, T.; Wimberger, K.; Amsuess, S.; Russold, M.F.; Baumgartner, W. An Insulated Flexible Sensor for Stable Electromyography Detection: Application to Prosthesis Control. *Sensors* **2019**, *19*, 961.
2. Yamagami, M.; Peters, K.; Milovanovic, I.; Kuang, I.; Yang, Z.; Lu, N.; Steele, K. Assessment of dry epidermal electrodes for long-term electromyography measurements. *Sensors* **2018**, *18*, 1269.

3. Posada-Quintero, H.F.; Rood, R.T.; Burnham, K.; Pennace, J.; Chon, K.H. Assessment of carbon/salt/adhesive electrodes for surface electromyography measurements. *IEEE journal of translational engineering in health and medicine* **2016**, *4*, 1–9.
4. Tabard-Fougère, A.; Rose-Dulcina, K.; Pittet, V.; Dayer, R.; Vuillerme, N.; Armand, S. EMG normalization method based on grade 3 of manual muscle testing: Within-and between-day reliability of normalization tasks and application to gait analysis. *Gait & posture* **2018**, *60*, 6–12.
5. Geng, W.; Du, Y.; Jin, W.; Wei, W.; Hu, Y.; Li, J. Gesture recognition by instantaneous surface EMG images. *Scientific reports* **2016**, *6*, 36571.
6. Khushaba, R.N.; Takruri, M.; Miro, J.V.; Kodagoda, S. Towards limb position invariant myoelectric pattern recognition using time-dependent spectral features. *Neural Networks* **2014**, *55*, 42–58.
7. Khushaba, R.N.; Al-Timemy, A.; Kodagoda, S.; Nazarpour, K. Combined influence of forearm orientation and muscular contraction on EMG pattern recognition. *Expert Systems with Applications* **2016**, *61*, 154–161.
8. Hakonen, M.; Piitulainen, H.; Visala, A. Current state of digital signal processing in myoelectric interfaces and related applications. *Biomedical Signal Processing and Control* **2015**, *18*, 334–359.
9. Tomczyński, J.; Mańkowski, T.; Kaczmarek, P. Localisation method for sEMG electrode array, towards hand gesture recognition HMI development. 2017 Signal Processing: Algorithms, Architectures, Arrangements, and Applications (SPA). IEEE, 2017, pp. 48–52.
10. Palermo, F.; Cognolato, M.; Gijsberts, A.; Müller, H.; Caputo, B.; Atzori, M. Repeatability of grasp recognition for robotic hand prosthesis control based on sEMG data. 2017 International Conference on Rehabilitation Robotics (ICORR). IEEE, 2017, pp. 1154–1159.
11. Zhai, X.; Jelfs, B.; Chan, R.H.; Tin, C. Self-recalibrating surface EMG pattern recognition for neuroprosthesis control based on convolutional neural network. *Frontiers in neuroscience* **2017**, *11*, 379.
12. Phinyomark, A.; Quaine, F.; Charbonnier, S.; Serviere, C.; Tarpin-Bernard, F.; Laurillau, Y. EMG feature evaluation for improving myoelectric pattern recognition robustness. *Expert Systems with applications* **2013**, *40*, 4832–4840.
13. Phinyomark, A.; Scheme, E. EMG pattern recognition in the era of big data and deep learning. *Big Data and Cognitive Computing* **2018**, *2*, 21.
14. Atzori, M.; Gijsberts, A.; Kuzborskij, I.; Elsig, S.; Hager, A.G.M.; Deriaz, O.; Castellini, C.; Müller, H.; Caputo, B. Characterization of a benchmark database for myoelectric movement classification. *IEEE Transactions on Neural Systems and Rehabilitation Engineering* **2014**, *23*, 73–83.
15. Atzori, M.; Gijsberts, A.; Castellini, C.; Caputo, B.; Hager, A.G.M.; Elsig, S.; Giatsidis, G.; Bassetto, F.; Müller, H. Electromyography data for non-invasive naturally-controlled robotic hand prostheses. *Scientific data* **2014**, *1*, 140053.
16. Pizzolato, S.; Tagliapietra, L.; Cognolato, M.; Reggiani, M.; Müller, H.; Atzori, M. Comparison of six electromyography acquisition setups on hand movement classification tasks. *PloS one* **2017**, *12*, e0186132.
17. Krasoulis, A.; Kyranou, I.; Erden, M.S.; Nazarpour, K.; Vijayakumar, S. Improved prosthetic hand control with concurrent use of myoelectric and inertial measurements. *Journal of NeuroEngineering and Rehabilitation* **2017**, *14*, 71. doi:10.1186/s12984-017-0284-4.
18. Cene, V.H.; Tosin, M.; Machado, J.; Balbinot, A. Open Database for Accurate Upper-Limb Intent Detection Using Electromyography and Reliable Extreme Learning Machines. *Sensors* **2019**, *19*, 1864.
19. Giordaniello, F.; Cognolato, M.; Graziani, M.; Gijsberts, A.; Gregori, V.; Saetta, G.; Hager, A.G.M.; Tiengo, C.; Bassetto, F.; Brugger, P.; others. Megane pro: myo-electricity, visual and gaze tracking data acquisitions to improve hand prosthetics. 2017 International Conference on Rehabilitation Robotics (ICORR). IEEE, 2017, pp. 1148–1153.
20. Khushaba, R.N.; Kodagoda, S. Electromyogram (EMG) feature reduction using mutual components analysis for multifunction prosthetic fingers control. 2012 12th International Conference on Control Automation Robotics & Vision (ICARCV). IEEE, 2012, pp. 1534–1539.
21. Du, Y.; Jin, W.; Wei, W.; Hu, Y.; Geng, W. Surface EMG-based inter-session gesture recognition enhanced by deep domain adaptation. *Sensors* **2017**, *17*, 458.

22. Amma, C.; Krings, T.; Böer, J.; Schultz, T. Advancing muscle-computer interfaces with high-density electromyography. *Proceedings of the 33rd Annual ACM Conference on Human Factors in Computing Systems*. ACM, 2015, pp. 929–938.
23. Gijssberts, A.; Atzori, M.; Castellini, C.; Müller, H.; Caputo, B. Movement error rate for evaluation of machine learning methods for sEMG-based hand movement classification. *IEEE transactions on neural systems and rehabilitation engineering* **2014**, *22*, 735–744.
24. Bi, L.; Guan, C.; others. A review on EMG-based motor intention prediction of continuous human upper limb motion for human-robot collaboration. *Biomedical Signal Processing and Control* **2019**, *51*, 113–127.
25. Tomczyński, J.; Kaczmarek, P.; Mańkowski, T. Hand gesture-based interface with multichannel sEMG band enabling unknown gesture discrimination. 2015 10th International Workshop on Robot Motion and Control (RoMoCo), 2015, pp. 52–57. doi:10.1109/RoMoCo.2015.7219713.
26. Tomczyński, J.; Mańkowski, T.; Kaczmarek, P. Localisation method for sEMG electrode array, towards hand gesture recognition HMI development. 2017 Signal Processing: Algorithms, Architectures, Arrangements, and Applications (SPA), 2017, pp. 48–52. doi:10.23919/SPA.2017.8166836.
27. Tomczyński, J.; Mańkowski, T.; Kaczmarek, P. Influence of sEMG electrode matrix configuration on hand gesture recognition performance. 2017 Signal Processing: Algorithms, Architectures, Arrangements, and Applications (SPA), 2017, pp. 42–47. doi:10.23919/SPA.2017.8166835.
28. Simonyan, K.; Zisserman, A. Very deep convolutional networks for large-scale image recognition. *arXiv preprint arXiv:1409.1556* **2014**.
29. Merletti, R.; Di Torino, P. Standards for reporting EMG data. *J Electromyogr Kinesiol* **1999**, *9*, 3–4.
30. Phinyomark, A.; Nuidod, A.; Phukpattaranont, P.; Limsakul, C. Feature extraction and reduction of wavelet transform coefficients for EMG pattern classification. *Elektronika ir Elektrotechnika* **2012**, *122*, 27–32.
31. Hudgins, B.; Parker, P.; Scott, R.N. A new strategy for multifunction myoelectric control. *IEEE Transactions on Biomedical Engineering* **1993**, *40*, 82–94.
32. Du, Y.C.; Lin, C.H.; Shyu, L.Y.; Chen, T. Portable hand motion classifier for multi-channel surface electromyography recognition using grey relational analysis. *Expert Systems with Applications* **2010**, *37*, 4283–4291.
33. Oskoei, M.A.; Hu, H. Support vector machine-based classification scheme for myoelectric control applied to upper limb. *IEEE transactions on biomedical engineering* **2008**, *55*, 1956–1965.
34. Phinyomark, A.; Phothisonothai, M.; Suklaead, P.; Phukpattaranont, P.; Limsakul, C. Fractal analysis of surface electromyography (EMG) signal for identify hand movements using critical exponent analysis. *International Conference on Software Engineering and Computer Systems*. Springer, 2011, pp. 703–713.
35. van Beek, N.; Stegeman, D.F.; Van Den Noort, J.C.; Veeger, D.H.; Maas, H. Activity patterns of extrinsic finger flexors and extensors during movements of instructed and non-instructed fingers. *Journal of Electromyography and Kinesiology* **2018**, *38*, 187–196.
36. Al-Timemy, A.H.; Bugmann, G.; Escudero, J.; Outram, N. Classification of finger movements for the dexterous hand prosthesis control with surface electromyography. *IEEE journal of biomedical and health informatics* **2013**, *17*, 608–618.
37. Jiang, M.; Wang, R.; Wang, J.; Jin, D. A method of recognizing finger motion using wavelet transform of surface EMG signal. 2005 IEEE Engineering in Medicine and Biology 27th Annual Conference. IEEE, 2006, pp. 2672–2674.
38. Tenore, F.V.; Ramos, A.; Fahmy, A.; Acharya, S.; Etienne-Cummings, R.; Thakor, N.V. Decoding of individuated finger movements using surface electromyography. *IEEE transactions on biomedical engineering* **2008**, *56*, 1427–1434.